



Microstructure and mechanical property of diamond-like carbon films with ductile copper incorporation



Wei Dai ^{a,*}, Aiyang Wang ^b, Qimin Wang ^a

^a School of Electromechanical Engineering, Guangdong University of Technology, Guangzhou 510006, PR China

^b Ningbo Key Laboratory of Marine Protection Materials, Ningbo Institute of Materials Technology and Engineering, Chinese Academy of Sciences, Ningbo 315201, PR China

ARTICLE INFO

Article history:

Received 29 December 2014

Accepted in revised form 15 April 2015

Available online 19 April 2015

Keywords:

Diamond-like carbon film

Cu doping

Residual stress

Elastic recovery

ABSTRACT

In this paper, a ductile and non-carbide former Cu was incorporated into diamond-like carbon (DLC) films to modify the microstructure and property of the films using a hybrid ion beam system comprising an ion beam source and a magnetron sputtering unit. The composition, microstructure, residual stress and mechanical property of the DLC films with Cu doping were characterized carefully using X-ray photoelectron spectroscopy, transmission electron microscopy and Raman spectroscopy, stress-tester, and nanoindentation as a function of Cu concentration. The results reveal that the doped Cu atoms had low solubility in the as-deposited DLC films. The maximum solubility was found to lie around 1.93 at.%. When the Cu concentration was lower than this solubility, the doped Cu atoms dissolved in the carbon matrix, and the film exhibited the typical amorphous structure of DLC and showed a low residual stress and high elastic recovery due to the dissolved Cu atoms which could play a role of the interstitial atoms for stress relaxation through the distortion of the atomic bond length and angle. As the doped concentration exceeded the solubility, Cu nanocrystalline was formed in the carbon matrix, which could significantly improve the elastic resilience of the film through strain release via sliding of the nanocrystalline in the amorphous carbon matrix. It is worth noting that when the doped Cu concentration approached the solubility limit, amorphous nano-clusters were formed in the carbon matrix due to the segregation of Cu, resulting in the decrease of the number of the interstitial atoms, and thus caused the increase in the residual stress and the decline in the elastic recovery.

© 2015 Elsevier B.V. All rights reserved.

1. Introduction

Diamond-like carbon (DLC) are well known for their outstanding properties such as high hardness and wear resistance, low friction coefficient, good anti-corrosion properties and bio-compatibility with the human body, and smooth surfaces. These excellent properties and their combination are very promising for a variety of technical applications such as applications in cutting tools and dies, magnetic data storage, micro-electromechanical devices, and biological implants [1–4]. However, a limited number of industrial utilization of DLC films were taken due to their low toughness and high compressive stress which tended to cause embrittlement and exfoliation of the films from substrates. Metal element doping has been considered to solve the problems of DLC films [5–7]. Generally, the metal atoms incorporated into the DLC matrix can form nano-clusters or bond with carbon atoms in case that the concentration of the doped metal is adequately high [8, 9]. These nanostructures embedded in the DLC matrix will significantly affect the microstructure and thus the properties of the DLC films.

So far numerous metallic components (Ti, Cr, Ag, Al etc.) have been used to modify DLC films [10–13]. Among these metal elements, the weak carbide former atoms, like Ag and Al, are incorporated into DLC and tend to form ductile metal phases in the carbon matrix, which have been expected to overcome the brittleness and improve the toughness of the DLC films [14,15]. Toughening significantly correlates with the composite structures of the doped metal atoms that can be nanocrystalline (or nanoparticle) or amorphous cluster in the amorphous carbon matrix. In case of nanocrystalline embedment, the toughening is obtained through strain release via sliding of the crystallites in the carbon matrix. In case of amorphous embedment, the toughening is realized through relaxation of stress via plastic deformation of the carbon phase [16]. This means that the toughening effect significantly depends on the existence form of the doped metal atoms in DLC films, which can be tailored by varying the nature and level of the doped metal atoms [14,16,17].

Copper is a ductile metal and non-carbide former, and has been considered to be a strong candidate element for reducing residual stress and improving the mechanical, tribological and biological properties of the DLC films [18–20]. In this paper, Cu was incorporated into the DLC films with different concentrations ranging from <1 up to 47 at.% using a hybrid ion beam system comprising an anode-layer linear ion

* Corresponding author.

E-mail address: popdw@126.com (W. Dai).

beam source (LIS) and DC magnetron sputtering unit. The evolution of the composition and microstructure of the Cu-DLC films were studied with increasing Cu concentration. The residual stress and mechanical properties including the elastic modulus, hardness and elastic resilience of the films were systematically investigated according to the microstructures of the films. The relationships between the microstructure, residual stress and mechanical properties were discussed in detail.

2. Experimental details

A series of Cu-DLC films were deposited on $525 \pm 15 \mu\text{m}$ thick silicon wafers using the hybrid ion beam system comprising LIS and DC magnetron sputtering unit equipped with a Cu target (99.99%). A schematic of the hybrid ion beam system and preparation process might be referred to in the previous work [21]. A gas mixture of C_2H_2 and Ar with a ratio of 65/15 (sccm) was introduced into the chamber as the carbon precursor and sputtering gas. Typical values of the work voltage and current of the linear ion source were $1600 \pm 100 \text{ V}$ and 0.2 A , respectively. DC power (under current control mode with a work voltage of $\sim 400 \text{ V}$) with various currents in the range of $0.5\text{--}3 \text{ A}$ was supplied to the magnetron sputtering unit to control the Cu target sputtering and thus adjust doped Cu concentration in the DLC films. The work pressure was kept at a constant of $\sim 0.5 \text{ Pa}$. A pulse negative bias voltage of -50 V (350 kHz, $1.1 \mu\text{s}$) was applied on the substrates. Two rounds of experiments have been carried out. The first round was done for measuring growth rates of the films. One the second one, the deposition times were adjusted according to the growth rates of the films to obtain a constant film thickness of $600 \pm 20 \text{ nm}$ for all samples.

A surface profilometer (Alpha-step IQ, US) was used to measure the thicknesses of the deposited films through a step between the films and Si wafers covered with a shadow mask. The composition and chemical bonds of the Cu-DLC films were analyzed using an X-ray photoelectron spectroscopy (XPS) (Axis ultraDLD) with Al (mono) $\text{K}\alpha$ irradiation at a pass energy of 160 eV . Before commencing the measurement, the sample surfaces were cleaned using an Ar^+ ion beam with an energy of 2 keV for 5 min to remove any contaminants. The Cu concentration in the films was calculated according to the relative Cu, C and O atomic ratios which were determined based on the atomic sensitivity factors and the relative area ratios of the peaks in XPS spectra of the films. For simplicity, the hydrogen concentration in the films was neglected due to the lack of signal intensity in the current XPS detection measurement. Transmission electron microscope (TEM, Tecnai F20, FEI company), operated at 200 keV with a point-to-point resolution of 0.24 nm , was employed to study the microstructures of the films. The TEM specimens were directly deposited on freshly cleaved single-crystal NaCl wafers with thicknesses of about 80 nm , and subsequently were peeled off by dissolving the NaCl wafers in deionized water. The carbon atomic bond details of the films were characterized using Raman spectroscopy with incident light from an Ar^+ laser at a wavelength of 514.5 nm .

The residual stresses of the films were calculated via the Stoney equation [22], where the curvature of the film/substrate composite was determined by a laser tester. The specimens for stress test were deposited on $285 \pm 5 \mu\text{m}$ thick silicon wafer strips of size $3 \text{ mm} \times 35 \text{ mm}$. The hardness and elastic modulus were measured by a nano-indentation technique (MTS-G200) in a continuous stiffness measurement mode with a maximum indentation depth of 500 nm . The characteristic hardness of the films was chosen in the depth of around $1/10$ th of the film thickness to minimize the substrate contribution. Six replicate indentations were operated for each sample.

3. Results and discussion

Fig. 1 shows the Cu concentration and the average growth rate of the films as a function of the sputtering current of the magnetron sputtering unit with Cu target. It can be seen that the Cu concentration of the deposited films continuously increased from 0.74 to $47.6 \text{ at.}\%$ as the

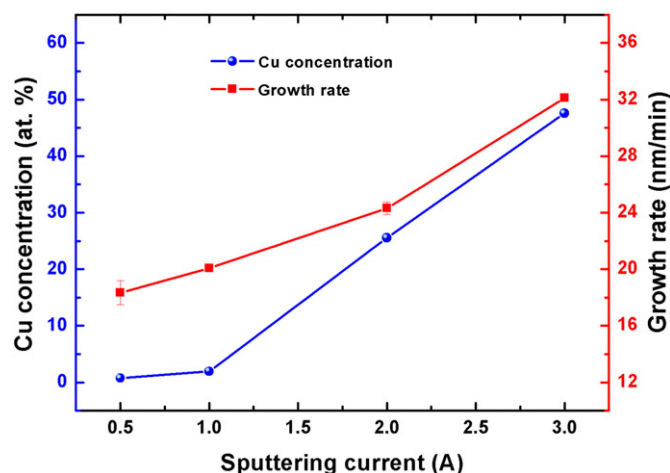


Fig. 1. Cu concentration and growth rate of the Cu-DLC films as a function of the sputtering current.

sputtering current increased from 0.5 to 3 A , indicating that the doped Cu concentration in films can be controlled through adjusting sputtering current. Note that the variation in the growth rate with the sputtering current was similar to that for the Cu concentration. The growth rate of the films increased from 11.5 to 16.2 nm/min as the current increased from 0.5 to 3 A . It seems that the magnetron sputtering would improve the growth rate of the films deposited by the hybrid ion beams, consisting with our previous results of other metal atoms doping DLC films [13,23].

The chemical bonds of the films with different Cu concentrations were analyzed by XPS and the corresponding high-resolution C 1s and Cu 2p core level spectra are shown in Fig. 2. It can be seen from Fig. 2(a) that, the intensity of the Cu 2p peak increased with increasing Cu concentration. All the spectra presented a symmetrical sharp peak centered at $\sim 932.2 \text{ eV}$, as expected for the $2p_{3/2}$ state of the metallic Cu. A small peak at 933.3 eV deconvoluted from the major peak could be assigned to Cu—O bonds. Fig. 2(b) illustrates the corresponding high resolution C 1s spectra of the films. The C 1s spectra could be deconvoluted into two strong and one weak intensity peaks around 284 eV , 285 eV and 286.8 eV , corresponding to $\text{sp}^2\text{—C}$, $\text{sp}^3\text{—C}$ and C—O bonds, respectively [24,25]. Because Cu is the non-carbide former, and immiscible with carbon, Cu—C bonds were not observed in present experiments. The presence of Cu—O and C—O peaks was due to the existence of oxygen, which may be attributed to two facts: the residual oxygen in the chamber and the sample exposure to air before XPS tests. The XPS results demonstrate that the main chemical form of the incorporated Cu in the DLC films is metallic state.

The bonding fractions of the sp^2 , sp^3 and C—O bonds in films were determined by the relative peak areas of the fitted peaks of Fig. 2(b) and are presented in Fig. 3. It can be seen that the sp^3 bond showed a sharp increase as Cu concentration increased from $0.74 \text{ at.}\%$ to $1.93 \text{ at.}\%$, followed by a relatively stable value of approximately 58% , while the sp^2 bond changed in the opposite trend simultaneously. The C—O bond had remained fairly constant with a value of approximately 2.5% . It was supposed that there was a critical Cu concentration between $0.74 \text{ at.}\%$ and $1.93 \text{ at.}\%$ at which a microstructure transition in the carbon atomic bonds (sp^2 and sp^3 bonds) occurred due to the Cu incorporation.

In order to obtain insight into the microstructure evolution of Cu-DLC films as a function of the doped Cu concentration, a TEM measurement was made. Fig. 4 shows the TEM micrographs and corresponding selected area electron diffraction (SAED) patterns of the DLC films with various Cu concentrations. It can be seen that the TEM picture and the corresponding magnified view of the film with $0.74 \text{ at.}\%$ Cu (Fig. 4(a) and (b)) exhibit dense and smooth granular contrasts, and

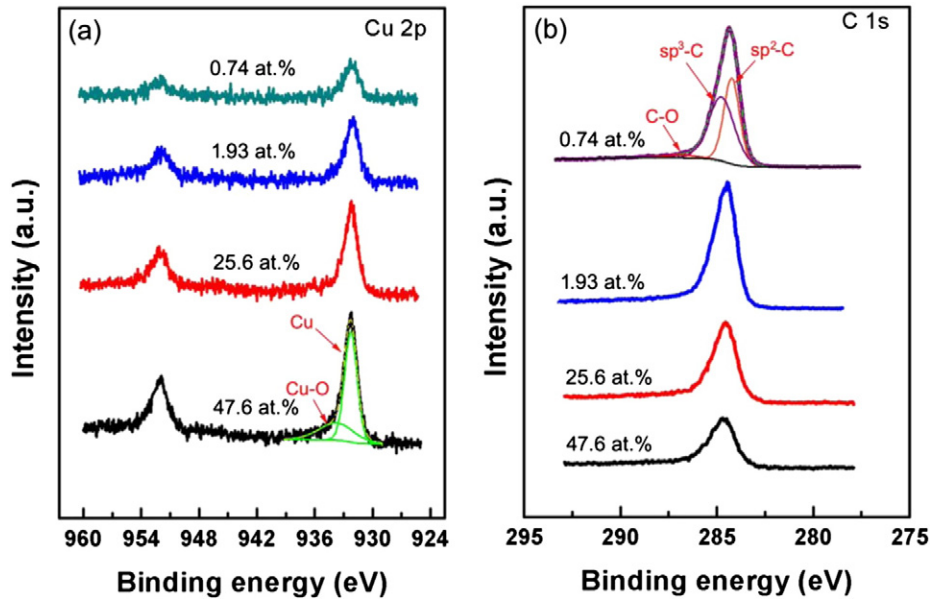


Fig. 2. (a) Typical XPS Cu 2p and (b) C 1s peaks of the films with various Cu concentrations.

the corresponding SAED inserted in Fig. 4(a) shows a broad and diffuse diffraction halo pointing out a typical amorphous feature, implying that the deposited film essentially formed a typical amorphous structure and the Cu atoms were uniformly distributed and dissolved in the amorphous carbon matrix. For the film with 1.93 at.% Cu, it can be seen that numerous isolated globular grains were presented, as shown in Fig. 4(b). The magnified view of Fig. 4(e) indicates that the globular grains (noted by the red circles) have typical sizes of approximately 3 nm in diameter. It was believed that these globular grains were perhaps the Cu-enrich nano-clusters, which were formed through the segregation of the doped Cu atoms as the doped concentration approached the solubility limit in the carbon matrix. However, the corresponding SAED also reveals a diffuse halo without any observable diffraction rings, indicating that the doped Cu existed as amorphous embedment. As the doped Cu concentration increased to 25.6 at.%, it is characteristic to note that numerous nanoparticles were presented in the film as shown in Fig. 4(c). A magnified image (Fig. 4(g)) reveals the clear lattice fringes of the nanoparticles (noted by the red circles) uniformly embedded in the DLC matrix, and the typical size of the crystal domains was 8–12 nm in diameter. Furthermore, the sharp crystalline diffraction rings observed in the inserted image of Fig. 4(c) indicate the existence

of polycrystalline phases, which were identified to be the (111), (200), and (220) reflections of the cubic (FCC) Cu structure [20]. In this case, it could be concluded that the Cu metallic crystalline phase was formed in the DLC film at relatively high concentration Cu doping. The TEM results indicate that the increased copper addition caused the microstructure of the DLC films to evolve from amorphous carbon structure with Cu solution, through amorphous composite structure with Cu amorphous nano-cluster embedment in carbon matrix, to nano-composite structure with nanocrystalline incorporating in amorphous carbon matrix. For this reason, we considered that the critical Cu concentration for the carbon atomic bond transition in XPS was the solubility limit of the Cu in the DLC films. Additionally, it can be seen that the Cu atoms had a relatively lower solubility of <1.93 at.% compared with other metal atoms such as Al, Cr and Ti in the DLC films that were also deposited by the hybrid ion beam system [5,13,23]. The difference of solubility of the doping metal atoms in a constant DLC matrix might be attributed to the nature of the doping metal atoms.

Raman spectroscopy is a popular and effective tool to characterize the carbon bonding in DLC films. Since the π states have a lower energy than the σ states and thus are more polarisable, the sp^2 sites consisting of two π orbits and two σ orbits have a 50–230 times larger Raman cross-section than sp^3 sites, which only contains four σ orbits [1]. Accordingly, the Raman spectrum of the DLC films is dominated by the sp^2 sites. Fig. 5(a) shows the representative Raman spectra of the Cu-DLC films with different Cu concentrations. A broad asymmetric Raman scattering band can be observed in the range from 1000 to 1700 cm^{-1} , representing the typical characteristic of DLC films [1]. The asymmetric Raman peaks can be fitted with two peaks: the G-peak around 1580 cm^{-1} and the D-peak around 1360 cm^{-1} , which correspond to the vibrations of C—C stretching and symmetric breathing vibration of the aromatic carbon rings, respectively [1,26]. Accordingly, the intensity ratio of D peak to G peak (I_D/I_G) is related to sp^2 clustering and increase as the sp^2 content increases [26,27]. Fig. 5(b) presents the ratio of I_D/I_G as a function of Cu concentration. It can be seen that the I_D/I_G showed a sharp decrease as Cu concentration increased from 0.74 to 1.93 at.%, implying that the sp^2 content of the films decreased. However, when the Cu concentration increased further to 47.6 at.%, the I_D/I_G exhibited a small dip, indicating that the sp^2 content of the films tended to increase. The change of the carbon atomic bond structure can be also illustrated by the FWHM of G peak (G_{FWHM}) which is expected to be sensitive to structural disorder that arose from bond angle and

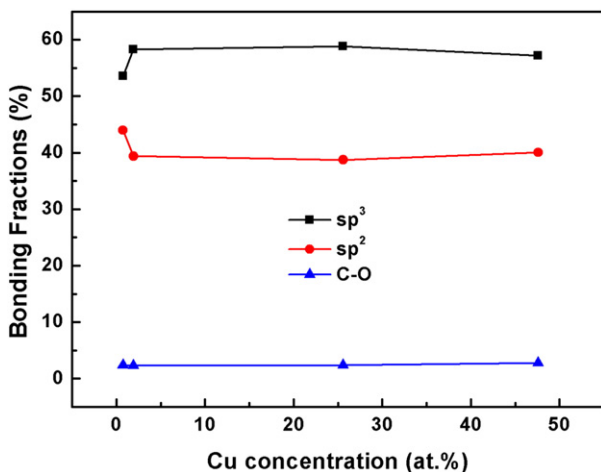


Fig. 3. Bonding fractions of the carbon bonds fitted in the XPS C 1s of Fig. 2(b).

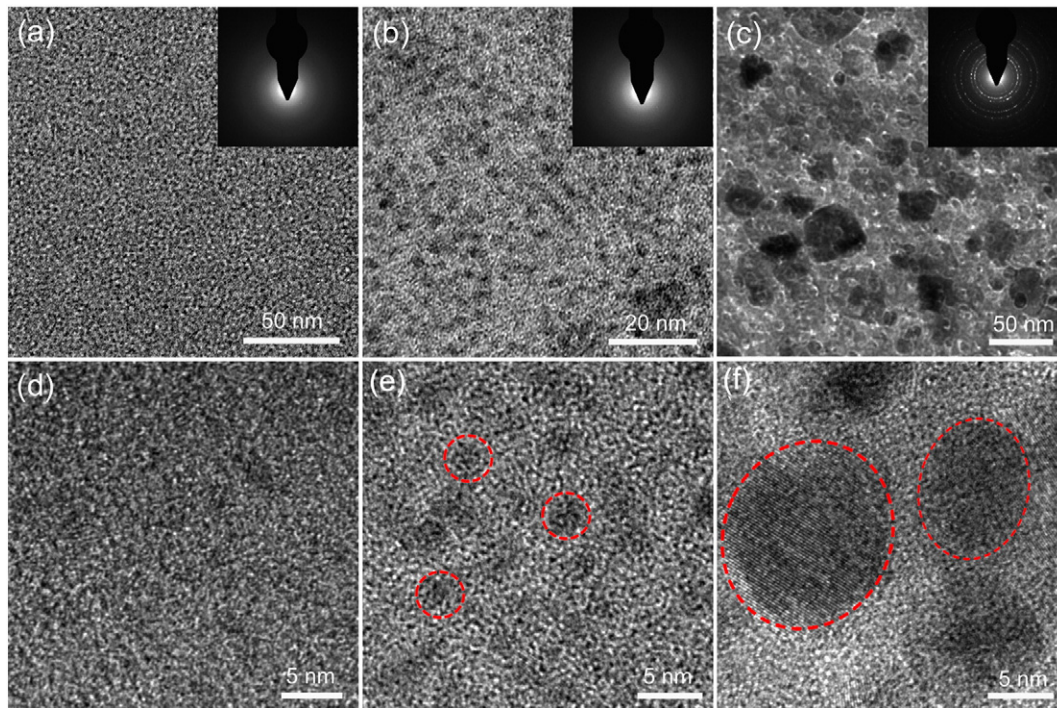


Fig. 4. TEM micrographs and corresponding SAED pattern of the Cu-DLC films with various Cu concentrations: (a) 0.74 at.%, (b) 1.93 at.% and (c) 25.6 at.%. (d), (e) and (g) are the corresponding high magnification micrographs of (a), (b) and (c), respectively.

bond length distortions, and a higher bond length and bond angle disorder lead to a higher G_{FWHM} [26]. The G_{FWHM} , as shown in Fig. 5(b), changed in the opposite trend simultaneously, which indicates that the structure disorder of the films increased as the Cu concentration increased from 0.74 to 1.93 at.%. In DLC films, the increase of disorder is linked to higher sp^3 content [26]. Accordingly, it can be seen that both the G_{FWHM} and I_D/I_G evolutions demonstrated that there was a major shift in carbon atomic bonds (sp^2 and sp^3 contents) of the DLC films when the Cu concentration increased from 0.74 to 1.93 at.%. This major shift point was attributed to the solubility limit of the doped Cu in the DLC films, which was proven by the XPS and TEM results above.

The residual stresses of the films were measured as a function of the Cu concentration, as shown in Fig. 6. A lower residual stress of 1.4 GPa was measured for the Cu-DLC film with Cu 0.74 at.% compared with that of the pure DLC film, which has a stress of about 2.7 GPa [13]. The residual stress of the films was increasing with increasing Cu concentration, and reached to 2.5 GPa, as the Cu concentration increased to 25.6 at.%, whereas it dramatically dropped down to 1 GPa as the Cu concentration increased further to 47.6 at.%.

It's worth to note that the variations in the film residual stress at different Cu concentrations were similar in profile to the G_{FWHM} values, indicating that the residual stress had a significant relationship with the degree of structure (bond length and bond angle) disorder of the film. The metal atoms dissolved in the amorphous carbon matrix without forming carbide bonds occupied interstitial positions between the carbon atoms, and thus reduced the bond length of carbon atoms. In addition, the atomic bond angles could easily distort around the interstitial metal atoms without inducing a significant increase in the elastic energy [28]. As a result, the DLC films got ordering with lower bond length and bond angle disorder under the distortion process. Meanwhile, the residual stress could, therefore, be significantly relaxed through the convenience of atomic bond distortion. As the structural and compositional analysis above, when the doped Cu concentration was 0.74 at.%, the doped Cu atoms were uniformly dissolved in the amorphous carbon matrix and thus could play the role of the interstitial metal atoms, and thus caused the decrease of the disorder degree and residual stress of

the DLC films. The consequence is similar to that seen in other metal-doped DLC films, where a small amount metal atoms were dissolved in the carbon matrix without forming carbide bonds and nano-clusters (or nanoparticles) can significantly reduce the residual stress of the DLC films [5,23,28]. For the films with Cu 1.93 at.%, however, the Cu was segregated from the carbon matrix to form nano-clusters since the Cu concentration was closed to the solubility level, and thus decreased the interstitial Cu atoms. As a result, the residual stress and degree of disorder (sp^3 content) in the film showed a sharp increase compared with that of the DLC films with Cu 0.74 at.%. As the doping Cu amount exceeded the solubility limit (>1.93 at.%), nanocrystalline was formed in the amorphous carbon matrix. The residual stress of the DLC films can be reduced via sliding of the crystallites. Accordingly, the residual stress began to decrease as the Cu concentration increased to 47.6 at.%.

The mechanical properties of hardness and elastic modulus of the Cu-DLC films were estimated as a function of the Cu concentration, as shown in Fig. 7. The variations in the film hardness and elastic modulus at different Cu concentrations were similar in profile to the residual stress, since both the residual stress and mechanical properties of the DLC films were highly dependent on the sp^3 -C bonding structures and the existence form of the doping Cu atoms. According to the XPS and Raman results, the low concentration (0.74 at.%) Cu doping caused the sp^3 bond content of the films to decrease. Accordingly, the film shows a relatively lower hardness of about 20 GPa compared with the pure DLC film which has a hardness of about 28 GPa. However, as the doping Cu concentration increased, the segregation of Cu atoms resulted in the increase of the sp^3 bond, which significantly contributed to the increase of the film hardness [1]. So the films displayed a high hardness value of around 27 GPa and an elastic modulus of 240 GPa at the Cu concentration of about 25.6 at.%. When the Cu concentration increased further (47.6 at.%), however, the large size of the nanocrystalline was formed in the film. The sliding of the crystallites and ductile Cu nanoparticles caused the film hardness to decrease sharply.

In order to investigate the elastic recovery properties of the films, typical nano-indentation load–displacement curves of the deposited

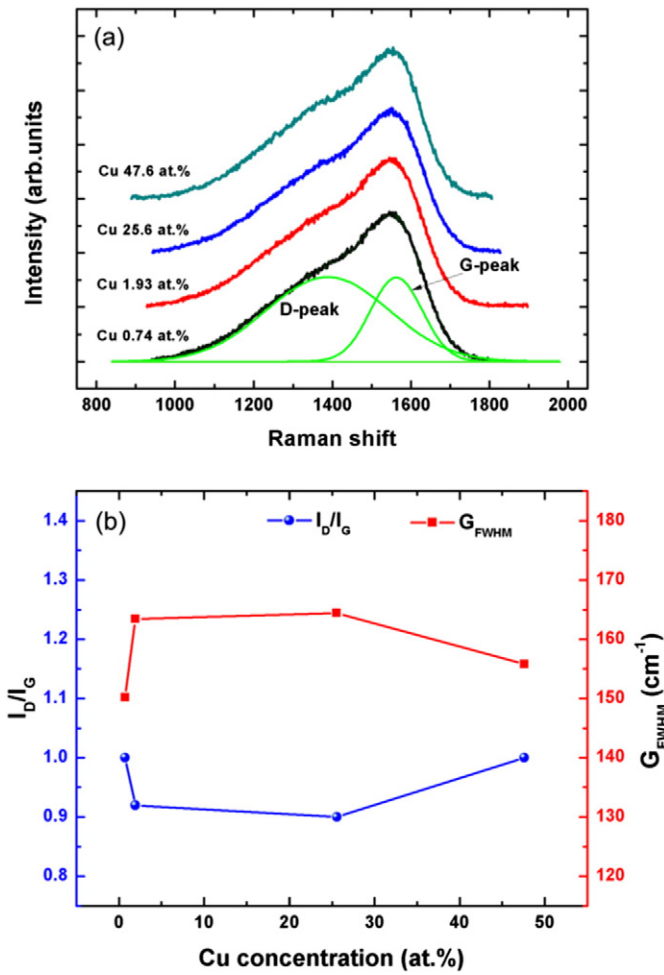


Fig. 5. (a) Representative Raman spectra, (b) corresponding I_D/I_G ratios and G_{FWHM} of the Cu-DLC films as a function of Cu concentration.

films are shown in Fig. 8(a). The elastic recovery R was defined as the ratio of the part of the indentation area that can be recovery (i.e., the elastic area) to the maximum indentation area [29]. The R values of the films deposited at various Cu concentrations are shown in Fig. 8(b). It can be seen that all the DLC films with Cu doping exhibited a relatively higher elastic recovery R than the pure DLC films, indicating

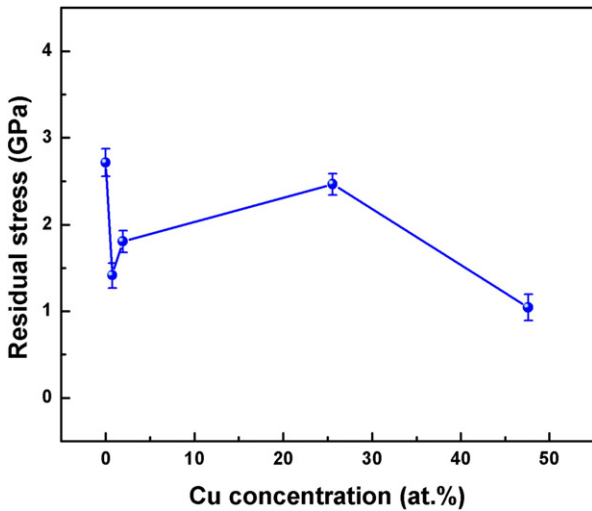


Fig. 6. Residual stress of the Cu-DLC films as a function of Cu concentration.

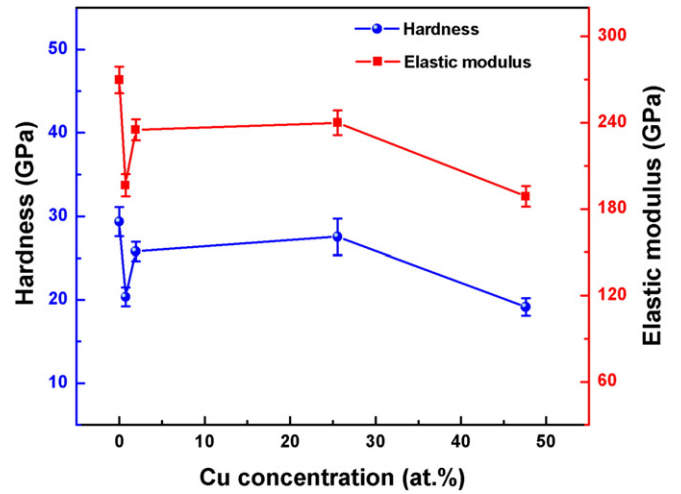


Fig. 7. Hardness and elastic modulus of the Cu-DLC films as a function of Cu concentration.

that the Cu incorporation could significantly improve the elastic resilience. It should be noted that the films with the Cu concentration of 1.93 at.% had the lowest R value of about 42% among the Cu-DLC films, and was close to the pure DLC film which has the R value of about 39%. The films with Cu 25.6 at.% showed the highest elastic recovery R of about 52%. At low doped concentration Cu (0.74 at.%), the increase

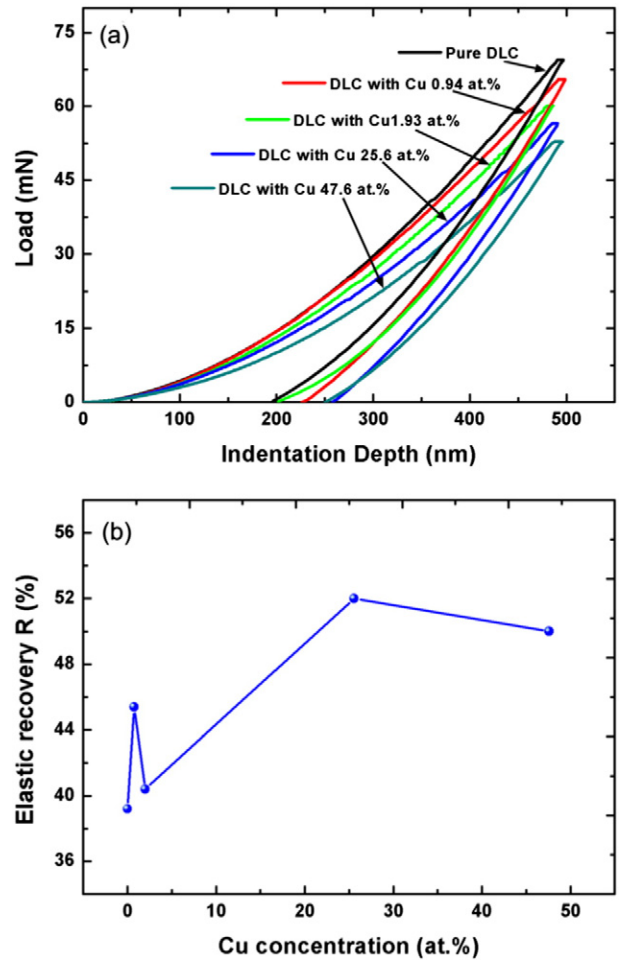


Fig. 8. (a) Typical nano-indentation load–displacement curves and (b) elastic recovery R of the DLC films with different Cu concentrations. The R was defined as the ratio of the part of the indentation depth that can be recovery to the maximum indentation depth in (a).

of the elastic recovery was mainly because of the relaxation of the film stress via Cu atom solution. As the Cu concentration increased to 1.93 at.%, however, the film stress got back to the high level due to the segregation of the doped Cu atoms (see Fig. 6), resulting in the reduction of the elastic recovery R. For the film with high doped Cu concentration, Cu metallic nanocrystallites (at Cu 25.6 and 47.6 at.%) were formed in the carbon matrix. The elastic resilience of the film can be improved through strain release via sliding of the crystallites in the amorphous carbon matrix. However, as the Cu concentration increased further (47.6 at.%), the large size of soft Cu nanoparticles caused the increase in the plastic and thus damaged seriously the elastic resilience of the film.

4. Conclusions

Cu-DLC films with various Cu concentrations were deposited by the hybrid ion beam system consisting of an anode-layer linear ion source and a DC magnetron sputtering source. Compositional and structural analysis showed that the maximum solubility of the doped Cu atoms in the films was proposed to lie around 1.93 at.%. As the doped Cu concentration increased from 0.74 to 47.6 at.%, the microstructures of the DLC films evolved from amorphous carbon structure with Cu solution, through amorphous composite structure with amorphous Cu nano-cluster embedment in carbon matrix, to nano-composite structure with nanocrystalline incorporating in amorphous carbon matrix. The residual stress and mechanical properties including hardness, elastic modulus and elastic recovery showed a significant relationship with the microstructure of the DLC films. The amorphous Cu-DLC film with a small amount of Cu dissolved in the carbon matrix displayed a low hardness and residual stress, but a high elastic recovery due to the dissolved Cu atoms which could play as the interstitial metal atoms, where the degree of disorder (sp^3 bond) and residual stress of the films can be reduced through the distortion of the atomic bond length and angle. The amorphous Cu-DLC film with amorphous nano-clusters embedding exhibited a high residual stress and hardness, but a low elastic recovery as the pure DLC showed due to the segregation of Cu atoms, which decreased the number of the interstitial Cu atoms, and thus caused the increase of the disorder degree and sp^3 bond. As a result, the residual stress of the films was increased while the elastic recovery was reduced. For the nanocomposite Cu-DLC film with Cu nanocrystalline embedment as the doped concentration exceeded the solubility limit, the

elastic recovery could be significantly improved through strain release via sliding of the nanocrystalline in the amorphous carbon matrix.

Acknowledgments

This work was financially supported by the projects of the National Natural Science Foundation of China (Grant No: 51405088) and the National Natural Science Foundation of Guangdong province (Grant No: 2014A030313516).

References

- [1] J. Robertson, *Mater. Sci. Eng. R* 37 (2002) 129.
- [2] K. Bewilogua, D. Hofmann, *Surf. Coat. Technol.* 242 (2014) 214.
- [3] J. Robertson, *Jpn. J. Appl. Phys.* 50 (2011) 01AF01.
- [4] C.A. Love, R.B. Cook, T.J. Harvey, P.A. Dearnley, R.J.K. Wood, *Tribol. Int.* 63 (2013) 141.
- [5] L. Ji, H. Li, F. Zhao, J. Chen, H. Zhou, *Diam. Relat. Mater.* 17 (2008) 1949.
- [6] W. Dai, G. Wu, A. Wang, *Diam. Relat. Mater.* 19 (2010) 1307.
- [7] L. Qiang, B. Zhang, Y. Zhou, J. Zhang, *Solid State Sci.* 20 (2013) 17.
- [8] V. Singh, J.C. Jiang, E.I. Meletis, *Thin Solid Films* 189 (2005) 150.
- [9] P. VijaiBharathy, D. Nataraj, P.K. Chu, H. Wang, Q. Yang, M.S.R.N. Kiran, J. Silvestre-Albero, D. Mangalaraj, *Appl. Surf. Sci.* 257 (2010) 143.
- [10] J. Cui, L. Qiang, B. Zhang, X. Ling, T. Yang, J. Zhang, *Appl. Surf. Sci.* 258 (2012) 5025.
- [11] Z. Wu, X. Tian, G. Gui, C. Gong, S. Yang, P.K. Chu, *Appl. Surf. Sci.* 276 (2013) 31.
- [12] N.K. Manninen, F. Ribeiro, A. Escudeiro, T. Polcar, S. Carvalho, A. Cavaleiro, *Surf. Coat. Technol.* 232 (2013) 440.
- [13] W. Dai, A. Wang, *J. Alloys Compd.* 509 (2011) 4626.
- [14] X. Yu, Z.W. Ning, M. Hua, C.B. Wang, *J. Adhes.* 89 (2013) 578.
- [15] S. Zhang, X.L. Bui, Y.Q. Fu, *Thin Solid Films* 467 (2004) 261.
- [16] S. Zhang, D. Sun, Y. Fu, H. Du, *Surf. Coat. Technol.* 198 (2005) 2.
- [17] S. Gayathri, N. Kumar, R. Krishnan, T.R. Ravindran, S. Dash, A.K. Tyagi, Baldev Raj, M. Sridharan, *Tribol. Int.* 53 (2012) 87.
- [18] N. Dwivedi, S. Kumar, H.K. Malik, C. Sree Kumar, S. Dayal, C.M.S. Rauthan, O.S. Panwar, *J. Phys. Chem. Solids* 73 (2012) 308.
- [19] Y. Pauleau, F. Thiery, V.V. Uglov, V.M. Anishchik, A.K. Kuleshov, M.P. Samtsov, *Surf. Coat. Technol.* 180–181 (2004) 102.
- [20] C.C. Chen, F.C.N. Hong, *Appl. Surf. Sci.* 242 (2005) 261.
- [21] W. Dai, H. Zheng, G. Wu, A. Wang, *Vacuum* 85 (2010) 231.
- [22] G.G. Stoney, *Proc. R. Soc. London, Ser. A* 82 (1909) 172.
- [23] W. Dai, P. Ke, M.W. Moon, K.R. Lee, A. Wang, *Thin Solid Films* 520 (2012) 6057.
- [24] N. Dwivedi, S. Kumar, S. Dayal Ishpal, C.M.S. Rauthan Govind, O.S. Panwar, *J. Alloys Compd.* 509 (2011) 1285.
- [25] N. Dwivedi, S. Kumar, H.K. Malik, C.M.S. Rauthan Govind, O.S. Panwar, *Appl. Surf. Sci.* 257 (2011) 6804.
- [26] C. Casiraghi, A.C. Ferrari, J. Robertson, *Phys. Rev. B* 72 (2005) 085401.
- [27] N. Dwivedi, E. Rismani-Yazdi, R.J. Yeo, P.S. Goohpattader, N. Satyanarayana, N. Srinivasan, B. Druz, S. Tripathy, C.S. Bhatia, *Sci. Rep.* 4 (2014) 5021.
- [28] A.Y. Wang, K.R. Lee, J.P. Ahn, J.H. Han, *Carbon* 44 (2006) 1826.
- [29] T.F. Page, S.V. Hainsworth, *Surf. Coat. Technol.* 61 (1993) 201.